 doi:10.20944/preprints202108.0073.v1

Article

How ultrasonic-assisted CO_2 EOR to unlock oils from unconventional reservoirs?

Hengli Wang [1,2], Leng Tian [1,2], Kaiqiang Zhang [3,*] Zongke Liu [1,2], Can Huang [1,2], Lili Jiang [1,2] and Xiaolong Chai [1,2]

[1] State Key Laboratory of Petroleum Resources and Prospecting, China University of Petroleum (Beijing), Beijing 102249, China;
[2] Department of Petroleum Engineering, China University of Petroleum (Beijing), Beijing 102249, China;
[3] Department of Chemical Engineering, Imperial College London, South Kensington Campus, London, SW7 2AZ, United Kingdom
* Leng Tian: tianleng2008@126.com; Tel.: 86-10-8973-3740; Kaiqiang Zhang: kaiqiang.zhang@imperial.ac.uk; Tel.: +44-(0)7742200006

Abstract: CO_2 enhanced oil recovery (EOR) has been proven its capability to explore the unconventional tight oil reservoirs and potential for geological carbon storage. Meanwhile, the extremely low permeability pores exaggerate the difficulty CO_2 EOR and geological storage processing in the actual field. This paper initiates the ultrasonic-assisted approach to facilitate the oil-gas miscibility development and finally contribute to unlock more tight oils. First, the physical properties of crude oil with and without ultrasonic treatments were experimentally analysed through gas chromatography (GC), Fourier-transform infrared spectroscopy (FTIR) and viscometer. Second, the oil-gas minimum miscibility pressures (MMPs) were measured from the slim-tube test and the miscibility developments with and without ultrasonic treatments were interpreted from the mixing-cell method. Third, the nuclear-magnetic resonance (NMR) assisted coreflood tests were conducted to physically model the recovery process in porous media and directly obtain the recovery factor. Basically, the ultrasonic treatment (40KHz and 200W for 8 hours) was found to substantially change the oil properties, with viscosity (at 60°C) reduced from 4.1 to 2.8mPa·s, contents of resin and asphaltene decreased from 27.94% and 6.03% to 14.2% and 3.79%, respectively. The FTIR spectrum shows the unsaturated C-H bond, C-O bond and C≡C bond in macromolecules were broken from ultrasonic, which caused the macromolecules (e.g., resin and asphaltenes) to be decomposed into smaller carbon-number molecules. Accordingly, the MMP was determined to be reduced from 15.8 to 14.9MPa from the slim-tube test and the oil recovery factor increased by over 10%. This study reveals the mechanisms of ultrasonic-assisted CO_2 miscible EOR in producing tight oils.

Keywords: Ultrasonic; Carbon dioxide; Enhanced oil recovery; Unconventional reservoirs

1. Introduction

The process of CO_2 flooding has proven to be an effective enhanced oil recovery (EOR) method in exploring low-permeability reservoirs [1-3]. The performance of CO_2 miscible flooding is much better then CO_2 immiscible because it can be dissolved in large quantities in crude oil and reduce the viscosity of the crude oil to improve the recovery in low-permeability reservoirs [4]. CO_2 is prone to gas channeling in low permeability reservoirs lead to the gas utilization rate is low, and the recovery rate of non-miscible flooding is much lower than that of miscible flooding [5-7]. However, due to the high minimum miscible pressure (MMP) of low permeability reservoirs in China, it is difficult to achieve miscible displacement [8]. Therefore, it is of practical and fundamental importance to study promotes CO_2 miscible flooding in low permeability reservoirs by ultrasonic wave.

Reducing MMP is a common method to realize CO_2 miscible flooding [9,10]. Purity of injected CO_2, viscosity of formation crude oil, formation temperature, composition of crude oil and pore size are all influencing factors of MMP [11-14]. The main direction of

reducing MMP between crude oil and CO_2 is to change the properties of carbon dioxide and crude oil [15-18]. During the experiment, CO_2 is usually injected into the core together with a certain ratio of liquefied gas, light components of crude oil or other miscible solvents (multi-component petroleum ether, methanol, ethanol, etc.) to promote the dissolution of CO_2 and crude oil to form a miscible displacement layer, reduce the MMP and improve oil recovery [19-21]. However, due to the consideration of safety and economy, 99.9% CO_2 is injected into the reservoir instead of co-injection of mixed solvents [22]. Therefore, the method of reducing the MMP by changing the nature of CO_2 still has great challenges in application.

For another thing, reducing MMP by adding chemicals to reduce the interfacial tension between crude oil and CO_2 to be an emerging technology that can improve oil recovery by up to 10% by converting the gas injection process from immiscible to miscible under the same reservoir conditions [23-25]. Mohamed Almobarak et al. confirmed that promising MMP reduction of 9% using 5wt% of the surfactant-based chemical (SOLOTERRA ME-6) at 373K by experiment [26]. Zhao found that the MMP can be reduced from 29.6MPa to 24.1MPa and the oil recovery efficiency can be increased by 10.3% with the size of citrate acid slug is 0.003PV into the core [27]. Luo found that in comparison to ethanol, Non-ionic Surfactant can significantly reduced the interfacial tension between CO_2 and crude oil, it at a dosage of 0.5wt% causes far higher reduction of the IFT than 20wt% pentane or 5wt% ethanol, the MMP and the first-contact miscibility pressures (P-max) of the crude oil/CO_2 systems were decreased from 19.1 and 43.0 to 13.8 and 19.0MPa [28]. The method of injecting chemicals can effectively reduce the MMP and improve the efficiency of CO_2 flooding, but the environmental protection restricts the large-scale application of chemicals.

In recent years, ultrasonic has been widely concerned by scholars due to its environmental friendliness and remarkable yield-increasing effect [29-32]. The heat generation, vibration, cavitation and emulsification of ultrasonic waves can reduce the viscosity of crude oil, capillary force and surface tension of oil and water in the process of water flooding, thereby improving the flow capacity of crude oil, which is the most important mechanisms that improve oil recovery factor [33-35]. Hossein Hamidi [36] verified an exciting finding that combining ultrasound application with CO_2 flooding in order to improve oil recovery could be of benefit by experimental. However, he only analyzed the effect of ultrasonic-assisted CO_2 flooding temperature on oil recovery through experimental methods and determined the optimal CO_2 injection rate. There was no in-depth analysis on the mechanism of EOR enhancement, and did not determine whether the effect of ultrasound could be reduced MMP made an explanation. So far, no attempts to determine the mechanism that ultrasonic action reduces MMP and enhances recovery by experiment.

The aim of the study is to analyze the effect of ultrasonic-assisted CO_2 flooding on MMP, pore structure and crude oil viscosity by combining slim tube experiment, NMR, infrared spectroscopy, viscosity test and displacement experiment, to explain the mechanism of enhanced oil recovery by ultrasonic-assisted CO_2 flooding, and to provide basic theoretical basis for the wide range application of ultrasonic-assisted CO_2 flooding in oil fields in the future.

2. Materials and Methods

2.1. Materials

The samples obtained for the present study were derived from tight sandstone samples sandwiched by the Upper Triassic Yanchang Formation in the JiYuan area located in the central Ordos Basin, China. The core with a length is 10.2cm, the diameter is 2.5cm, the permeability is 1.56mD, and the porosity is 10.3%. It belongs to low permeability reservoir according to permeability. The oil samples is collected from the surface degassing crude oil of Chang 6 low permeability reservoir in Ordos Basin. The density and viscosity of the oil sample are measured to be 895 kg/m^3 and 3.8mPa·s at 60 ℃ (Reservoir

 doi:10.20944/preprints202108.0073.v1

temperature) and atmospheric pressure, respectively. The purity of CO_2 used in the experiment was 99.9%.

2.2. Equipment Setup

2.2.1. Subsubsection

The oil viscosity, component of oil and functional group were measured by viscometer, gas chromatography and Fourier-transform infrared spectroscopy (FTIR). The viscometer used in this experiment is VISCOlab PVT produced by Cambridge Viscometer Co., Ltd., USA. The maximum test pressure is 138MPa, the maximum temperature is 190 ℃, the measurement range is 0.02-10000CP, and the measurement error is 1%. Total hydrocarbon analysis was performed using Agilent 7890 gas chromatography-mass spectrometer. The stationary phase of the high resolution chromatographic column is a quartz capillary column formed by the crosslinking of polymethylsiloxane. The column length is 35m-50m, the inner diameter is 2.2cm-2.5cm, the operating temperature is higher than 320 °C, and the column efficiency is higher than 3000 theoretical plate/m. Fourier infrared spectrum instrument is an FT-IR model produced by SPECIM Company in Finland, with a resolution of 4 cm^{-1} and a spectral range of 7800-350 cm^{-1}.

2.2.2. Slim-tube test

In this research, the slim-tube apparatus was used to determine the MMP of the oil and CO_2 at the constant reservoir temperature. The experimental apparatus is shown in Fig. 1, which mainly include: (1) ISCO pump (Quizix5000, Broken Arrow, OK, USA), it can provide the maximum displacement pressure of 70MPa for the experiment. (2) Slim tube (from Hai'an, Nantong, China), it has been filled by 160mesh quartz sand and with an internal diameter of 5 mm, a length of 20 m, the permeability is 1200mD and the porosity is 22.8%. (3) Ultrasonic bath (from Beijing China), the ultrasonic waves with a frequency of 40KHz and a power of 200W was emitted by transducer transmitted to the slim-tube through the water in the water tank. On the one hand, water is the medium of ultrasonic transmission. On the other hand, the ultrasonic bath can control the temperature of water and keep the experimental temperature constant. (4) Observation window, it's used to look at miscible states. (5) Backpressure valve (HY-2, Nantong, China), it is used to stabilize the back pressure to ensure that the displacement pressure difference is stable. (6) Hand pump, it is used to provide pressure to the backpressure valve. (7) Measuring device, the produced oil was monitored and measured by an electronic balance with an accuracy of 0.0001g.

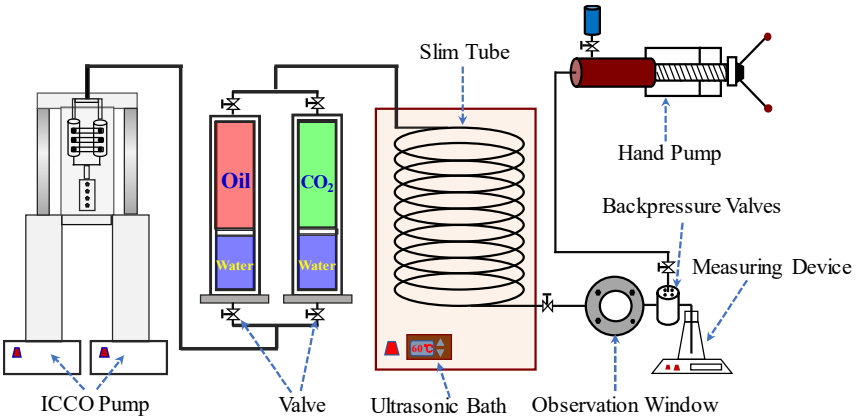

Figure 1. Experimental installation diagram of thin tube.

 doi:10.20944/preprints202108.0073.v1

2.2.3. NMR and CO_2 flooding

The experimental setup for ultrasonic assisted CO_2 flooding and on-line NMR testing is shown in Fig. 2. It consists of four subsystems, i.e., displacement subsystem with nuclear magnetic resonance, ultrasonic generation subsystem, measuring subsystem and assistant subsystem. In the displacement subsystem, ICSO pump (Broken Arrow, OK, USA) can provide the maximum displacement pressure of 70MPa for the experiment, the pressure passed from the pump ICSO pushes the fluid in the container (Hai´an, Nantong, China) to the core holder (from Hai´an, Nantong, China, with diameter of 26mm, length of 90mm-150mm) and flows through the core to the vent. Two hand pumps (P5, 35MPa, 80°C, Oxford, UK) provide confining pressure to core holder and pressure to backpressure valve (HY-2, Nantong, China) respectively. The NMR instrument (from Oxford instruments, UK. the radio frequency is distributed in a range of 1-30MHz with a control precision of 0.1MHz. Besides, the echo time is set to be 0.12ms, waiting time is 1.125s for measurement, and the scanning number is 32) is used to detect the spectrum of transversal relaxation time (T_2) to analyze the recovery of CO_2 flooding and residual oil distribution. The ultrasonic generation subsystem consists of ultrasonic generator (HC-SG-202000, from Hangzhou, China, with 40KHz and 50W) and transducer. The measuring subsystem consists of a high-precision electronic balance and a gas flow meter (50scm, ALICAT, USA). As an assistant subsystem, thermotank (from Hai´an, Nantong, China) can maintain the experimental temperature within the range of room temperature to 120℃, with an error of ±1℃ .

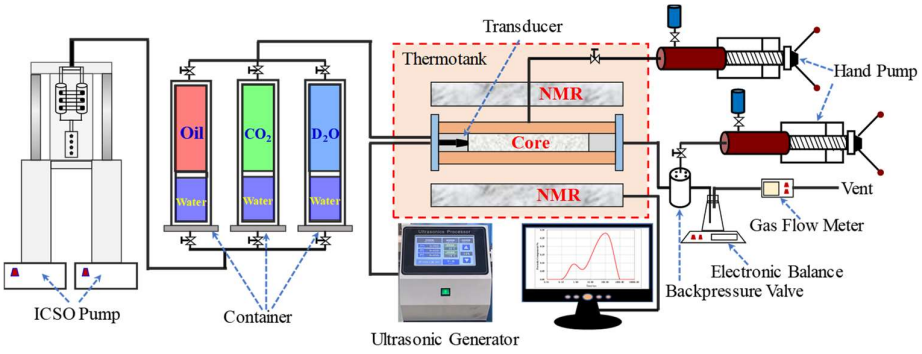

Figure 2. Diagram of ultrasonic-assisted CO_2 displacement device.

2.3. Procedure

2.3.1 Physical property measurement

The changes of oil viscosity, group component, composition and functional groups after ultrasonic treatment were measured. 1L crude oil was averagely divided into two parts with the same viscosity, composition and functional group. One part of them is used for viscosity test, gas chromatography test and infrared spectroscopy test. The other part of the crude oil is sealed in the glass beaker, and then the beaker is completely submerged under the water surface of the ultrasonic bather. The oil was treated 8 hours by ultrasonic wave with 40KHz and 50W used for viscosity test, gas chromatography test and infrared spectroscopy test.

The viscosity-temperature curves of crude oil viscosity changing with temperature were obtained in the temperature range of 20°C-60°C. Group components include saturated hydrocarbons, aromatic hydrocarbons, resins, asphaltenes (SARA). The filtrate formed by asphaltene precipitation in crude oil was separated by silica alumina column with n-hexane, and then saturated hydrocarbon, aromatic hydrocarbon and resin components were leached out by dichloromethane, anhydrous ethanol and chloroform, respectively. The contents of four kinds of components were obtained by weighing the weight of the solvent after volatilization.

During the analysis of crude oil by gas chromatography, the gasified oil sample was first slowly passed through capillary column with carrier gas to separate light hydrocarbons less than C_8 and alkanes from C_8-C_{40}. The concentration of each component was detected by flame ionization detector and the mass fraction of each component was calculated by area normalization method. The capillary column temperature was stabilized at 40°C for 10 minutes and then raised to 320°C at 5°C/min. The temperature of vaporization chamber and detection chamber was kept at 330°C and the split ratio was controlled at 1:40-1:120. The linear velocity of helium is 20cm/s, the flow rate of hydrogen gas is 30ml/min and the flow rate of air is 300ml/min. After the instrument was stabilized, 0.2μL-1.0μL samples were extracted with a microinjector. At the same time, the programmed temperature was started and the chromatographic processor was used to record the chromatogram and original data.

After adjusting the sensitivity, parameter mode, gain and velocity of the infrared spectrometer, the infrared analysis begins. First, the potassium bromide slide was cleaned with anhydrous ethanol and a background data was measured for later reference. Then the crude oil was evenly smeared on the slide, the C-H vibration response of the absorption spectrum was adjusted to 100%, and the absorption peak heights of methyl, methylene, aromatic ring and carbon and oxygen functional groups were taken as their relative contents for quantitative calculation.

2.3.2 Slim-tube test

Once the slim tube is saturated with the crude oil sample at 60℃, CO_2 is introduced to displace the oil at an injection rate of 0.2cm^3/min. The volume of oil produced after the CO_2 injection volume reaches 1.2PV at the displacement pressure of 12MPa, 14MPa, 15MPa, 16MPa, 18MPa and 20MPa was recorded respectively. The displacement pressure difference has been 0.5MPa. Keep the experimental material, temperature, pressure same and repeat the above experimental procedure with the ultrasonic bath machine was open, the MMP of ultrasonic assisted CO_2 flooding was measured.

2.3.3 NMR and CO_2 flooding

Step #1: after the gas permeability measurement of core samples is completed, the sample was vacuum pressurized (15MPa) saturated brine and placed in the core holder in Fig. 2 for NMR test.

Step #2: the sample was dried and the brine made of deuterium oxide with purity of 99.99% was saturated by vacuum pressure (15MPa). Then the crude oil was saturated by displacement method with the displacement pressure was 16MPa, the displacement pressure difference was 1MPa, and the confining pressure was 18MPa, then the core sample was placed in the core gripper and aged with confining pressure for 120 hours for NMR test.

Step #3: The samples was replaced with CO_2 at a displacement pressure of 15MPa, displacement pressure difference of 1MPa and confining pressure of 17MPa. Record oil and gas production data respectively. When the injection volume of CO_2 reached 1.6PV, the displacement experiment was stopped for NMR test.

Step #4: the residual oil in the pores was thoroughly washed by the solution prepared with alcohol and benzene at a volume ratio of 1:3, then dried at 105°C for 12 hours. Repeat step #3.

Step #5: open the ultrasonic generator, repeat step #3, measure ultrasonic assisted CO_2 displacement recovery.

3. Results and Discussion

3.1 Oil Physical Properties

Table 1 shows the changes of group composition after ultrasonic treatment for 8 hours. It can be seen from the table that the contents of saturated hydrocarbon and aromatic hydrocarbon in crude oil increased by 9.8% and 6.2% after ultrasonic treatment, and

 doi:10.20944/preprints202108.0073.v1

the contents of resin and asphaltene decreased by 13.7% and 2.2%, respectively. The experimental results show that the crude oil treated by ultrasonic is cracked, and the heavy components such as gum and asphaltene in crude oil are transformed into light components such as saturated hydrocarbons and aromatic hydrocarbons.

Table 1. SARA of ultra-oil samples before and after ultrasonic treatment.

	Saturated hydrocarbon/%	Aromatic hydrocarbon/%	Resin/%	Asphaltene/%
Without ultrasonic	52.38	13.65	27.94	6.03
With ultrasonic	62.15	19.87	14.20	3.79

Figure 3 is the result of gas chromatography. The results show that after ultrasonic treatment for 8 hours, the molar percentage of C_{25}-C_{30+} in crude oil decreases, that is to say, the content of heavy hydrocarbon molecules decreases, and the decrease of C_{30+} component is the largest, from 5.6% to 5.0%. With the decrease of C atom number, the decrease of molar percentage is also reduced. But C_{12}-C_{24} mole percentage increases, C_3-C_{11} change irregularly. The experimental results show that the heavy hydrocarbon molecules (C_{25+}) in crude oil components can be decomposed into medium hydrocarbon molecules (C_{12}-C_{24}) by ultrasound. Studies have shown that the MMP is related to the content of heavy hydrocarbon molecules in crude oil. The greater the content of heavy hydrocarbon molecules is, the greater the MMP is [37-39]. This is one of the important reasons why ultrasound can reduce MMP.

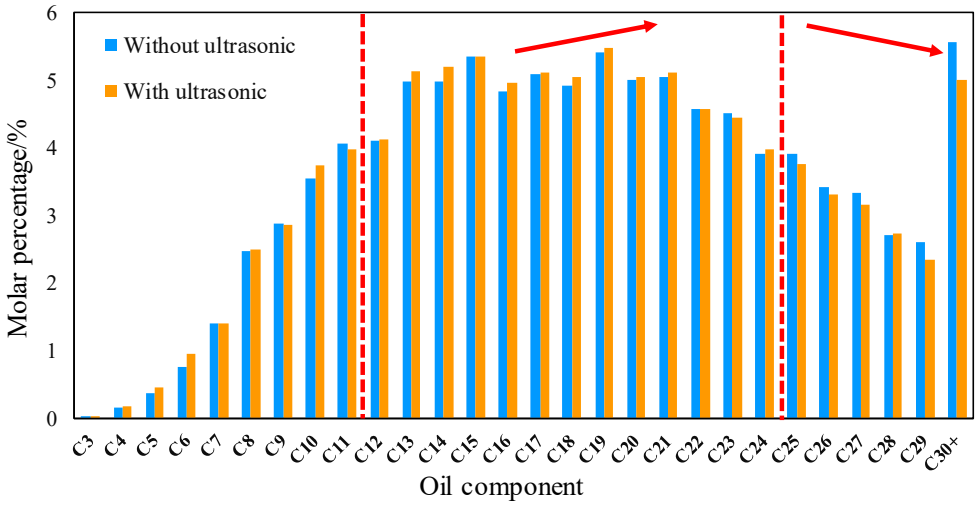

Figure 3. Result of gas-chromatography experiment. (the mole fraction of C_{25+} goes down, the mole fraction of $C_{12\text{-}24}$ goes up).

Cavitation is the main mechanism of ultrasonic changing crude oil composition. Cavitation gathers ultrasonic energy in the tiny space of crude oil to form tiny bubbles called the nucleus. When the cavitation nucleus disappears, it produces huge pressure and releases a lot of heat. The high temperature and high pressure around the cavitation core and the accompanying severe mechanical shear can improve the activity of crude oil macromolecules, start the thermal decomposition reaction similar to combustion, and thus break the crude oil macromolecules into small molecules [40,41].

Infrared spectroscopy is one of the main methods for identifying functional groups and molecular structures of substances. The infrared spectrum is the characteristic absorption peak of typical hydrocarbon (functional group). The functional groups in crude oil

Preprints (www.preprints.org) | NOT PEER-REVIEWED | Posted: 3 August 2021 doi:10.20944/preprints202108.0073.v1

samples can be sensitively studied by Fourier transform infrared spectroscopy, and the relative concentration (ratio) of each functional group can be obtained by the relative quantitative calculation of aromatic rings, methylene and methyl according to the peak height or area. By comparing and analyzing the infrared spectra of crude oil before and after the reaction, the changes of various functional groups and their relative contents in the samples can be revealed [42,43].

The FTIR spectrum covers the range of 4000-400cm^{-1}. The region in 700-820cm^{-1} presents the out-plane bending vibration of C-H structural and the region in 1000-1100cm^{-1} shows the stretching vibration of C-O structure. There are double peaks that the peak areas are equal with value are 1365cm^{-1} and 1395cm^{-1} in the range of 1340-1410cm^{-1}, which presents the in-plane bending vibration of C-H structural [44]. In the range of 1560-1620cm^{-1}, 1620-1680cm^{-1} shows the stretching vibration of C=C groups, interestingly, 1560-1620cm^{-1} represents the C=C stretching vibration of aromatic molecules, while 1620-1680cm^{-1} is the C=C structure of alkenes [45]. The range of 2010-2070cm^{-1} and 2920-2980cm^{-1} indicate the stretching interval of C≡C and -CH_2 respectively. In the range of 3300-3500cm^{-1} shows the stretching vibration of C-H [46,47].

Figure 4 shows the test results of FTIR. The red line represents the infrared absorption spectrum of crude oil without ultrasonic treatment, and the blue line represents the infrared absorption spectrum of crude oil after 8 hours of ultrasonic treatment. The origin 2018 software was used to segment fit the peak values of infrared spectrum, and the area of each peak was obtained to represent the number of corresponding functional groups. The results are shown in Table 2. After ultrasonic treatment, the peak areas of both in-plane bending vibration and out-of-plane bending vibration of saturated C-H increased, and in addition, the peak areas of unsaturated C-H stretching vibration decreased, that is to say, the unsaturated C-H bond was broken and turned into a saturated C-H bond due to ultrasonic treatment. Because unsaturated C-H bond mainly exists in colloid and asphaltene, it can be inferred that the unsaturated C-H bond of colloid and asphaltene is mainly cracked by ultrasonic, which is converted to saturated C-H bond by hydrogenation reaction. The decrease of the number of C-O functional groups indicates that the C-O bond in crude oil is broken by ultrasonic, and hydrogen atoms replace oxygen atoms to bond with carbon atoms, which is one of the reasons for the increase of the number of C-H functional groups. With the ultrasonic treatment, the number of C≡C bond decreases, and the C=C bone in both aromatic ring and olefin increases, indicating that C≡C bond was cracked into C=C bond by ultrasonic treatment. In summary, the ultrasonic action makes the C-H bond, C-O bond and C≡C bond of resin and asphaltene in crude oil crack to generate the C-H bond and C=C bond of saturated hydrocarbon and aromatic hydrocarbon.

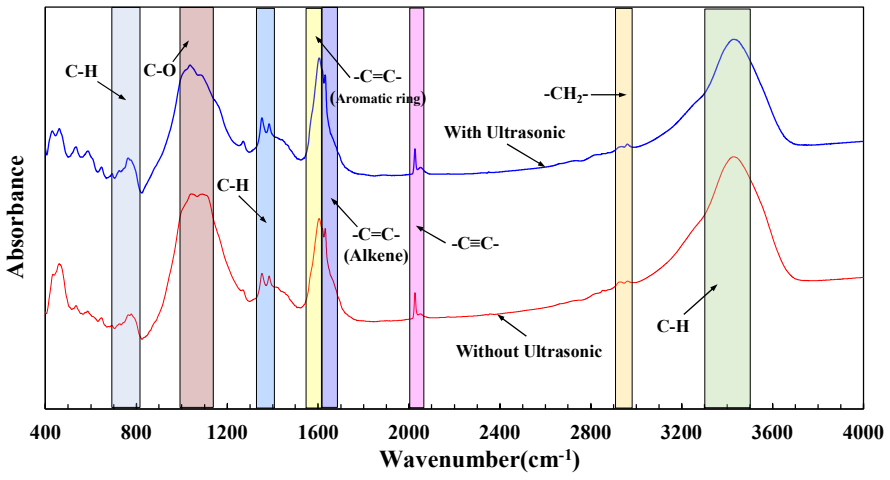

Figure 4. Result of FTIR.

 doi:10.20944/preprints202108.0073.v1

Table 2. Number of functional group of ultra-oil samples before and after ultrasonic treatment.

Functional groups	C-H (out-plane bending vibration)	C-O	C-H (in-plane bending vibration)	C=C (Aromatic ring)	C=C (Alkene)	C≡C	-CH_2	C-H (stretching vibration)
Range/cm^{-1}	700-820	1000-1100	1340-1410	1560-1620	1620-1680	2010-2070	2920-2980	3300-3500
Area (Without ultrasonic)	23.27	78.56	20.58	8.78	15.11	4.38	1.82	96.3
Area (With ultrasonic)	26.74	70.21	21.35	9.46	16.07	4.07	1.81	88.7

The viscosity test results in Figure 5 show that the viscosity of crude oil decreases with the increase of temperature. When the temperature is less than 44℃, the viscosity decreases greatly with the increase of temperature, and then the viscosity decreases gently. After being treated by ultrasonic wave, the viscosity of crude oil decreases from 88.6mPa·s to 53.1mPa·s at 20℃, and decreased from 4.1mPa·s to 2.5mPa·s at 60℃. Resin and asphaltene are the most important factors to controlling the viscosity of crude oil. With asphaltenes as the core, resins are attached to asphaltenes to form aggregates or micelles which are dispersed in the dispersion medium composed of light components and some resins. The connection between resin and asphaltenes were destroyed by ultrasonic treat, which makes the micelle structure loose and reduces the cohesion between crude oil molecules, which is shown by the decrease of the crude oil viscosity. The crude oil without ultrasonic treatment contains 33.97% of the heavy components of resin and asphaltene, which showed the characteristics of high viscosity. After ultrasonic treatment, the total content of resin and asphaltene in crude oil decreased to 17.99%, which was the main reason for ultrasonic to reduce the viscosity of crude oil.

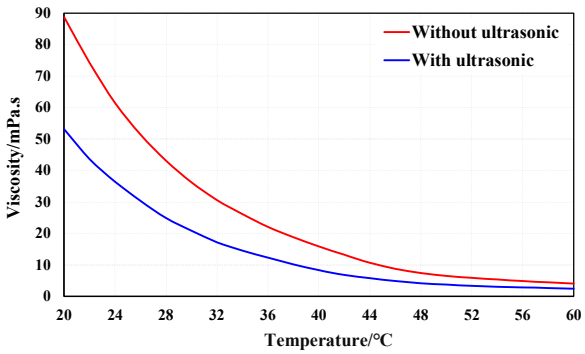

Figure 5. Viscosity-temperature curve of ultra-oil samples before and after ultrasonic treatment. (in the absence of ultrasonic effect the oil viscosity was 88.6mPa·s at 20℃ and 4.1mPa·s at 60℃, the viscosity of crude oil was 53.1mPa·s at 20℃ and 2.5mPa·s at 60℃ after 8 hours of ultrasonic treatment.).

3.2. Miscibility Development

The experimental results of the slim-tube are shown in Figure 6. It can be seen that the experimental results of the tube can be approximated by two straight lines. The pressure corresponding to the intersection point of the straight line is the MMP. The MMP decreased from 15.9MPa without ultrasonic to 14.8MPa with ultrasonic, indicating that

Preprints (www.preprints.org) | NOT PEER-REVIEWED | Posted: 3 August 2021 doi:10.20944/preprints202108.0073.v1

ultrasonic treatment can reduce the MMP between CO_2 and crude oil. With ultrasonic wave can improve oil recovery by 8.9%, and the pressure for displacement of 12MPa. The increase of recovery rate decreases gradually with the increase of injection pressure, especially when the pressure is greater than the MMP, the increase of recovery rate decreases rapidly. Only 0.6% recovery can be increased by ultrasonic when the displacement pressure is 20MPa. It can be seen that the ultrasonic is the best to improve the development of CO_2 immiscible flooding because the recovery ratio of miscible flooding in the slim tube experiment is greater than 90%, and there is little residual oil used to improve the recovery ratio.

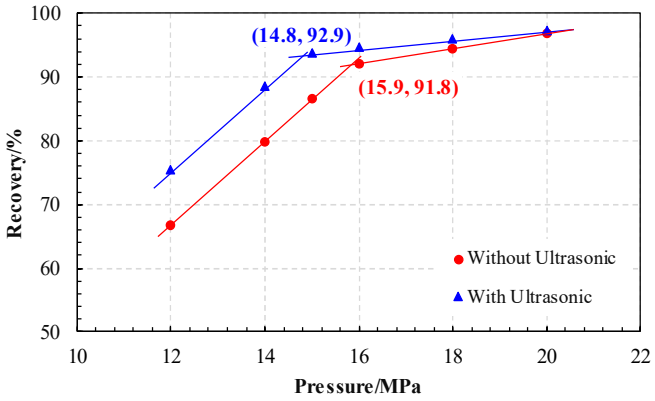

Figure 6. Result of slim-tube test. (the MMP decreased from 15.9MPa without ultrasonic to 14.8MPa after ultrasonic treatment for 8 hours).

A large number of studies have shown that the MMP is associated with the purity of injected CO_2, crude oil composition, reservoir temperature and the size of pore and throat, especially most affected by the crude oil composition [48-52]. The MMP increased with the increase of the molar fraction of C_{11}-C_{19} and C_{20+} in crude oil, and they are almost linearly correlated with MMP. The difference is that MMP increases more with the increase of C_{20+}, meaning that the influence of the molar content of C_{20+} on MMP is more intense [53]. There are many empirical formulas for calculating the MMP considering the reservoir temperature, crude oil composition and gas composition [54-58]. Among them, the method of characteristic theory and the mixing-cell method are one of the most classical methods for calculating MMP. Dangke Ge et al. [59] propose a prediction model of CO_2-oil MMP considering multi-stage contact based on method of characteristic theory and the mixing-cell method. This method is used to calculate the MMP of CO_2-oil system before and after ultrasonic treatment in this paper. The pressure corresponding to a zerolength tie line is MMP which acquired by power-law extrapolation, but the extrapolation can also lead to the error of prediction. Therefore, Dangke Ge et al. proposed to approximate the MMP with the minimum value of the characteristic curve. The calculation formula for the minimum value of the characteristic curve is:

$$V_{min} = 0.0017 * \mathrm{T} + 0.057 * C_{7-15} + 0.174 * C_{16-26} - 0.0405 * C_{27+} \quad (1)$$

where *Vmin* is the minimum value. *T* is reservoir temperature. $C_{7\text{-}15}$ is mole fraction. $C_{16\text{-}26}$ is mole fraction. C_{27+} is mole fraction. Table 3 shows the calculation parameters and results, the minimum value of the characteristic curve without ultrasonic effect is 0.203, and the minimum value of the characteristic curve with ultrasonic effect is 0.212.

Table 3. Calculation parameters and results.

	T/℃	$C_{7\text{-}15}$/%	$C_{16\text{-}26}$/%	C_{27+}/%	V_{min}
Without ultrasonic	60	33.82	50.67	15.51	0.203
With ultrasonic	60	34.32	54.44	11.24	0.212

 doi:10.20944/preprints202108.0073.v1

As shown in Figure 7, mix a cell G filled with injected gas and a cell O filled with crude oil in a certain proportion (typically 50% each). At a fixed temperature and pressure, the composition of the equilibrium gas phase Y_1 and liquid phase X_1 is calculated by negative flash, and the first contact is completed by adding four units of crude oil O and injected gas G. For the second contact, the equilibrium gas phase cell Y_1 continues to mix with the crude oil cell O in the front, and the equilibrium liquid phase cell X_1 continues to mix with the injected gas cell G in the rear, producing X_{21}, Y_{21}, X_{22} and Y_{22}. Two groups of equilibrium gas-liquid compositions were obtained by two negative flash calculations, there are 6 cells including of crude oil and injected gas. In this way, 2n+2 cells should be obtained when the nth contact is completed. Line length can be presented by equilibrium components X_i, Y_i:

$$TL = \sqrt{\sum_{i=1}^{N_c}(x_i - y_i)^2} \quad (2)$$

where TL is the tie-line length, N_C is the number of components and X_i and Y_i are liquid and gas equilibrium compositions, respectively

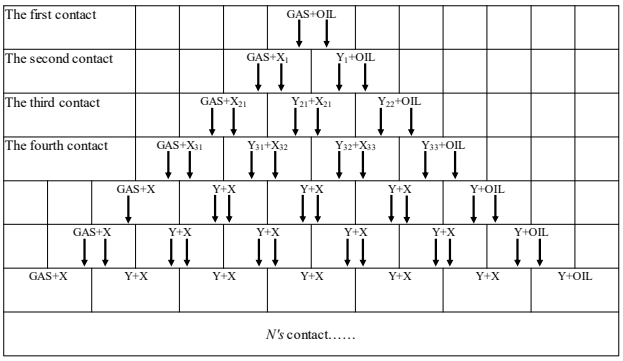

Figure 7. Mixing-cell processes [59].

Firstly, at a fixed reservoir temperature and an initial pressure less than MMP, the gas-liquid equilibrium is calculated by PR equation of state as shown in Figure 7. After 200 contact times, the gas-liquid tie-line length (TL) of each group was calculated, and the minimum tie-line length (MTL) was selected. Then slightly increase the pressure value, repeat the above steps, calculate the MTL under the pressure. Taking the pressure as the abscissa and the MTL as the ordinate, the MTL under all pressure is drawn in the rectangular coordinate system. Figure 8 shows the relationship between the MTL and pressure. It can be seen from the figure that the MTL decreases with the increase of pressure. When the pressure is the same, the MTL with ultrasonic is smaller than that without ultrasonic.

According to Equation 1, the MTL of CO_2-oil system without ultrasonic is 0.120, and the corresponding MMP is 16.7MPa. The MTL of CO_2-oil system assisted by ultrasonic is 0.212, and the MMP is 15.7MPa. Obviously, the MMP of CO_2-oil system decreases after adding ultrasonic, indicating that ultrasonic effect can promote the CO_2-oil system to reach the miscible state.

 doi:10.20944/preprints202108.0073.v1

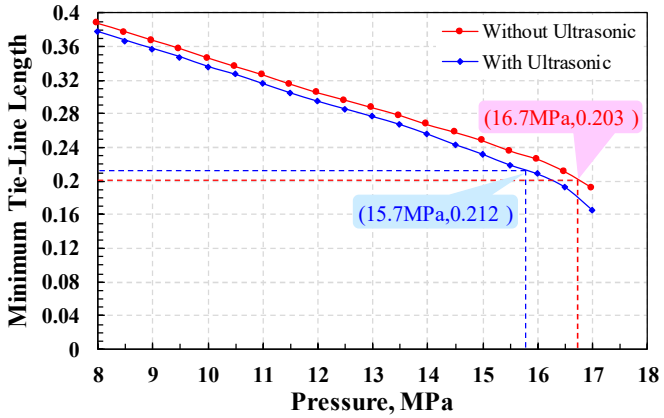

Figure 8. The relationship between MTL with pressure. (with the increase of pressure, the MTL decreases. Under the same pressure condition, the MTL of ultrasonic treatment is always smaller than that of non-ultrasonic treatment).

3.3 Oil Recovery

Figure 9 shows the NMR results of CO_2 flooding. The four curves represent the cumulative T_2 spectra of 100% saturated water, saturated oil to bound water, residual oil in CO2 flooding without ultrasonic and residual oil with ultrasonic-assisted CO_2 flooding, respectively. The 100% saturated water reflects the original porosity of the core is 7.7%, and the cumulative T_2 spectrum curve from saturated oil to irreducible water reflects a porosity of 6.2% in the core due to the D_2O filled in the core before saturated oil shielding the vibration signal of hydrogen atoms. Similarly, the accumulated T_2 spectrum after the CO_2 displacement without ultrasonic wave reflects a porosity of 2.8% for the residual oil. After the ultrasonic CO_2 displacement, the porosity of the residual oil was 2.1%. According to the information provided in the Figure 9, the initial oil saturation is 80.5%, the residual oil saturation is 36.7% and the recovery is 54.3% without ultrasonic CO_2 displacement. The residual oil saturation of ultrasonic-assisted CO_2 flooding was 27.3%, and the recovery factor was 65.9%. Compared with other conditions unchanged, the recovery rate of CO_2 flooding increases by 11.7% with ultrasonic. One of the most important reasons is that in the absence of ultrasonic effect, the MMP obtained by the thin tube experiment is 15.9 MPa, the CO_2-oil system is immiscible due to the displacement pressure of 15 MPa is less than the MMP. Ultrasonic-assisted CO_2 displacement reduced the MMP to 14.8 MPa, which promotes the CO_2-oil system to miscible state, so the recovery is greatly improved.

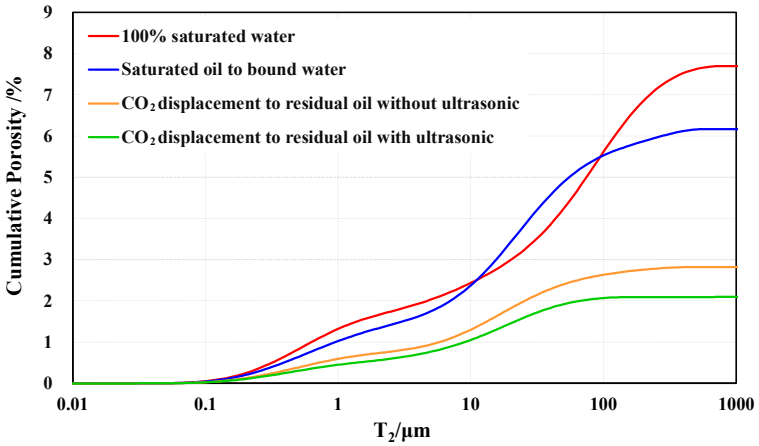

Figure 9. The accumulation T_2 curve of CO_2 flooding. (ϕ=7.7%, porosity of saturated oil is 6.2%, porosity of residual oil without ultrasonic is 2.8% and porosity of residual oil with ultrasonic is 2.1%).

4. Conclusions

1. 8 hours after ultrasonic processing of crude oil viscosity is reduced by 39%. The reason is that under the effect of ultrasonic, the unsaturated C-H bond in resin and asphaltene molecules in crude oil was destroyed and saturated C-H bond was generated through hydrogenation reaction. The C-O bond was broken and the oxygen atom was replaced by hydrogen atom to form C-H bond. The C≡C bond was destroyed to form C=C bond in aromatic rings and olefins. Under the influence of ultrasonic cavitation, the mole fraction of C_{25+} molecules decreases with the destruction and recombination of these chemical bonds, and the mole fraction of C_{12-24} molecules increases, indicating that macromolecules such as resin and asphaltene are decomposed into small molecules with relatively small carbon atoms, resulting in the decrease of their contents by 13.7% and 2.2%, respectively.

2. As the viscosity of crude oil decreased and the mole fraction of C_{12-24} increased after ultrasonic treatment for 8 hours, the MMP of CO_2-oil system decreased from 15.9 MPa to 14.8 MPa in the thin tube experiment, and the MMP calculated by mixing-cell method decreased from 16.7 MPa to 15.7 MPa.

3. The displacement pressure is stable at 15MPa. and the reduction of the MMP promoted the miscible phase of the CO_2-oil system. Recovery increased by 11.7% from 54.3% for non-miscible flooding to 65.9% for miscible flooding. This result indicates that the ultrasonic assisted CO_2 flooding can effectively reduce the MMP and improve the recovery.

Author Contributions: Conceptualization, Hengli Wang and Leng Tian; methodology, Hengli Wang; software, X.X.; validation, Zongke Liu; resources, Can Huang; data curation, Lili Jiang; writing—original draft preparation, Hengli Wang; writing—review and editing, Kaiqiang Zhang; visualization, Xiaolong Chai; project administration, Leng Tian. All authors have read and agreed to the published version of the manuscript.

Funding: This research was funded by National Natural Science Foundation of China (Grant No.: 51974329).

Conflicts of Interest: The authors declare no conflict of interest.

References

1. Dara S, Lindstrom M, English J, Bonakdarpour A, Wetton B, Wilkinson DP. Conversion of saline water and dissolved carbon dioxide into value-added chemicals by electrodialysis. *Journal of CO_2 Utilization* **2017**, 19, 177–184.
2. Abbasi J, Ghaedi M, Riazi M. A new numerical approach for investigation of the efects of dynamic capillary pressure in imbibition process. *Journal of Petroleum Science and Engineering* **2018**, 162, 44–54.
3. Huang X, Qi Z, Yan W, Yuan Y, Tian J, Qin T. Functions of capillary pressure and dissolution in the CO_2 flooding process in low permeability reservoirs. *Journal of Petroleum Exploration and Production Technology* **2020**, 10, 1881–1890.
4. Su X, Yue X. Mechanism study of the relation between the performance of CO_2 immiscible flooding and rock permeability. *Journal of Petroleum Science and Engineering* **2020**, 195, 107891.
5. Gao C, Zhao M, Wang J, Zong C. Performance and gas breakthrough during CO_2 immiscible flooding in ultra-low permeability reservoirs. *Petroleum Exploration and Development* **2014**, 41, 88-95.
6. Hao S, Yang Z, Li X , Peng Y , Lin M , Zhang J , Dong Z. CO_2-responsive agent for restraining gas channeling during CO_2 flooding in low permeability reservoirs. *Fuel* **2021**, 292, 120306.
7. Wang Y, Shang Q, Zhou L, Jiao Z. Utilizing macroscopic areal permeability heterogeneity to enhance the effect of CO_2 flooding in tight sandstone reservoirs in the Ordos Basin. *Journal of Petroleum Science and Engineering* **2021**, 196, 107633.
8. Chen X, Li Y, Tang X, Qi H, Sun X, Luo J. Effect of gravity segregation on CO_2 flooding under various pressure conditions: Application to CO_2 sequestration and oil production. *Energy* **2021**, 226, 120294.
9. Zhao Y, Fan G, Song K, Li Y, Chen H, Sun H. The experimental research for reducing the minimum miscibility pressure of carbon dioxide miscible flooding. *Renewable and Sustainable Energy Reviews* **2021**, 145, 111091.
10. Zhang K, Jia N, Zeng F, Li S, Liu L. A review of experimental methods for determining the oil-gas minimum miscibility pressures. *Journal of Petroleum Science and Engineering* **2019**, 183, 106366.
11. Chen H, Zhang C, Jia N, Ian D, Yang S, Yang Y. A machine learning model for predicting the minimum miscibility pressure of CO_2 and crude oil system based on a support vector machine algorithm approach. *Fuel* **2021**, 290, 120048.
12. Ge D, Cheng H, Cai M, Zhang Y, Dong P. A new predictive method for CO_2-Oil minimum miscibility pressure. *Geofluids* **2021**, 8868529.
13. Zhang K, Meng Z, Liu L. Factorial two-stage analyses of parameters affecting the oil-gas interface and miscibility in bulk phase and nanopores. *Journal of Colloid and Interface Science* **2019**, 555, 740–750.

14. Zhang K, Jia N, Li S, Liu L. Thermodynamic phase behaviour and miscibility of confined fluids in nanopores. *Chemical Engineering Journal* **2018**, 351, 1115–1128.
15. Gunde A C, Bera B, Mitra S K. Investigation of water and CO_2 (carbon dioxide) flooding using micro-CT(micro-computed tomography) images of Berea sandstone core using finite element simulations. *Energy* **2010**, 35, 5209–5216.
16. Song Z, Li Z, Yu C. D-optimal design for rapid assessment model of CO_2 flooding in high water cut oil reservoirs. *Journal of Nature Gas Science and Engineering* **2014**, 21, 764–771.
17. Choubineh A, Helalizadeh A, Wood DA. The impacts of gas impurities on the minimum miscibility pressure of injected CO_2-rich gas-crude oil systems and enhanced oil recovery potential. *Petroleum Science* **2019**, 16, 117-126.
18. Ghorbani M, Momeni A, Safavi S, Gandomkar A. Modified vanishing interfacial tension(VIT) test for CO_2-oil minimum miscibility pressure(MMP) measurement. *Journal of Nature Gas Science and Engineering* **2014**, 20, 92–98.
19. Zhang C, Xi L, Wu P, Li Z. A novel system for reducing CO_2-crude oil minimum miscibility pressure with CO_2-soluble surfactants. *Fuel* **2020**, 281, 118690.
20. Yang Z, Wu W, Dong Z, Lin M, Zhang S, Zhang J. Reducing the minimum miscibility pressure of CO_2 and crude oil using alcohols. *Colloids and Surfaces A–Physicochemical and Engineering Aspects* **2019**, 568, 105–112.
21. Liu J, Sun L, Li Z, Wu X. Experimental study on reducing CO_2–Oil minimum miscibility pressure with hydrocarbon agents. *Energies* **2019**, 12, 1975.
22. Zhao Y, Song K, Fan G, Pi Y, Liu L. The experiment for reducing the minimum miscible pressure of crude oil and carbon dioxide system with eater compounds. *Acta Petrolei Sinica* **2017**, 38, 1066–1072.
23. Wang X, Gu Y. Oil recovery and permeability reduction of a tight sandstone reservoir in immiscible and miscible CO_2 flooding processes. *Industrial & Engineering Chemistry Research* **2011**, 50, 2388–2399.
24. Cao M, Gu Y. Physicochemical characterization of produced oils and gases in immiscible and miscible CO_2 flooding processes. *Energy & Fuels* **2013**, 27, 440–453.
25. Cao M, Gu Y, Oil recovery mechanisms and asphaltene precipitation phenomenon in immiscible and miscible CO_2 flooding processes. *Fuel* **2013**, 109, 157–166.
26. Mohamed A, Wu Z, Matthew B. Myers, Colin D. W, Nasser S. A, Liu Y, Renke R, Ali S, Xie Q. Chemical-assisted minimum miscibility pressure reduction between oil and methane. *Journal of Petroleum Science and Engineering* **2021**, 196, 108094.
27. Zhao Y, Fan G, Li Y, Zhang X, Chen H, Sun H. Research for reducing minimum miscible pressure of crude oil and carbon dioxide and miscible flooding experiment by injecting citric acid isopentyl ester. *Arabian Journal of Chemistry* **2020**, 13, 9207–9215.
28. Luo H, Zhang Y, Fan W, Nan G, Li Z. Effects of the non-ionic surfactant (CiPOj) on the interfacial tension behavior between CO_2 and crude oil. *Energy & Fuels* **2018**, 32, 6708–6712.
29. Bjorndalen N, Islam MR, The effect of microwave and ultrasonic irradiation on crude oil during production with horizontal well. *Journal of Petroleum Science and Engineering* **2004**, 43, 139–150.
30. Mohsin M, Meribout M, Oil–water de-emulsification using ultrasonic technology. *Ultrasonics Sonochemistry* **2015**, 22, 573579.
31. Abramov VO, Abramova AV, Bayazitov VM, Altunina LK, Gerasin AS, Pashin DM, Mason TJ, Sonochemical approaches to enhanced oil recovery. *Ultrasonics Sonochemistry* **2015**, 25, 76–81.
32. Abramov VO, Mullakaev MS, Abramova AV, Esipov IB, Mason TJ. Ultrasonic technology for enhanced oil recovery from failing oil wells and the equipment for its implemention. *Ultrasonics Sonochemistry* **2013**, 20, 1289–1295.
33. Hamidi H, Mohammadian E, Asadullah M, Azdarpour A, Rafati R. Effect of ultrasound radiation duration on emulsification and demulsification of paraffin oil and surfactant solution/brine using hele-shaw models. *Ultrasonics Sonochemistry* **2015**, 6, 428–436.
34. Hamidi H, Rafati R, Junin R, Manan M, Busra N. A technique for evaluating the oil/heavy-oil viscosity changes under ultrasound in a simulated porous medium. *Ultrasonics* **2013**, 54, 655–662.
35. Mohammadian E, Junin R, Rahmani O. Effects of sonication radiation on oil recovery by ultrasonic waves stimulated waterflooding. *Ultrasonics* **2013**, 53, 607–614.
36. Hossein H, Amin SH, Erfan M, Roozbeh R, Amin A, Panteha G, Peter O, Tobias N, Aaron Z. Ultrasound-assisted CO_2 flooding to improve oil recovery. *Ultrasonics Sonochemistry* **2017**, 35, 243–250.
37. Czarnota R, Janiga D, Stopa J, Wojnarowski P, Kosowski P. Minimum miscibility pressure measurement for CO_2 and oil using rapid pressure increase method. *Journal of CO_2 Utilization* **2017**, 21, 156–161.
38. Czarnota R, Janiga D, Stopa J, Wojnarowski P. Determination of minimum miscibility pressure for CO_2 and oil system using acoustically monitored separator. *Journal of CO_2 Utilization* **2017**, 17, 32–36.
39. Ren B, Duncan IJ. Maximizing oil production from water alternating gas (CO_2) injection into residual oil zones: The impact of oil saturation and heterogeneity. *Energy* **2021**, 222, 119915.
40. Gopinath R, Dalai AK, Adjaye J. Effects of ultrasound treatment on the upgradation of heavy oil. *Energy & Fuels* **2006**, 20, 271–277.
41. Liu J, Yang FK, Xia JY, Wu FP, Pu CS. Mechanism of ultrasonic physical-chemical viscosity reduction for different heavy oils. *ACS Omega* **2021**, 6, 2276–2283.
42. Chen B, Han XX, Jiang XM. In situ FTIR analysis of the evolution of functional groups of oil shale during pyrolysis. Energy & *Fuels* **2016**, 30, 5611–5616.
43. Shaw A, Zhang XL. Density functional study on the thermal stabilities of phenolic bio-oil compounds. *Fuel* **2019**, 225, 115732.

44. Wartini N, Brendan PM, Budiman M. Rapid assessment of petroleum-contaminated soils with infrared spectroscopy. *Geoderma* **2017**, 289, 150–160.
45. Zhang W, Ning Z, Cheng Z, Wang Q, Wu X, Huang L. Experimental investigation of the role of DC voltage in the wettability alteration in tight sandstones. *Langmuir* **2020**, 36, 11985–11995.
46. Lee Y, Chung H, Kim N. Spectral range optimization for the near-infrared quantitative analysis of petrochemical and pPetroleum products: naphtha and gasoline. *Applied Spectroscopy* **2006**, 60, 892–897.
47. Nataly J. Galán-Freyle, María L. Ospina-Castro, Alberto R. Medina-González, Reynaldo Villarreal-González, Samuel P. Hernández-Rivera, Leonardo C. Pacheco-Londoño. Artificial intelligence assisted mid-infrared laser spectroscopy in situ detection of petroleum in soils. *Applied Science* **2020**, 10, 1319.
48. Cao M, Gu Y. Temperature effects on the phase behaviour, mutual interactionsand oil recovery of a light crude oil–CO_2 system. *Fluid Phase Equilibria* **2013**, 356, 78–89.
49. Liao C, Liao X, Chen J, Ye H, Chen X, Wang H. Correlations of minimum miscibility pressure for pure and impure CO_2 in low permeability oil reservoir. *Journal of the Energy Institute* **2014**, 87, 208–214.
50. Lai F, Li Z, Hu X. Improved minimum miscibility pressure correlation for CO_2 flooding using various oil components and their effects. *Journal of Geophysics and Engineering* **2017**, 14, 331–340.
51. Zhang K, Jia N, Liu L. CO_2 storage in fractured nanopores underground: Phase behaviour study. *Applied energy* **2019**, 238, 911–928.
52. Zhang K, Jia N, Zeng F, Li S, Liu L. A review of experimental methods for determining the Oil-Gas minimum miscibility pressures. *Journal of Petroleum Science and Engineering* **2019**, 183, 106366.
53. LeRoy W. Holm, Virgil A. Josendal. Effect of oil composition on miscible-type displacement by carbon dioxide. *Society of Petroleum Engineers Journal* **1982**, 22, 87–98.
54. Chen H, Li B, Ian D, Moayad E, Liu X. Empirical correlations for prediction of minimum miscible pressure and near-miscible pressure interval for oil and CO_2 systems. *Fuel* **2020**, 278, 118272.
55. Chen G, Fu K, Liang Z, Teerawat S, Li C, Paitoon T, Raphael I. The genetic algorithm based back propagation neural network for MMP prediction in CO_2-EOR process. *Fuel* **2014**, 126, 202–212.
56. Chen G, Gao H, Fu K, Zhang H, Liang Z, Paitoon T. An improved correlation to determine minimum miscibility pressure of CO_2–Oil system. *Green Energy and Environment* **2018**, 5, 97–104.
57. Zhang K, Gu Y. Two different technical criteria for determining the minimum miscibility pressures (MMPs) from the slim-tube and coreflood tests. *Fuel* **2015**, 161, 146–156.
58. Zhang K, Gu Y. New qualitative and quantitative technical criteria for determining the minimum miscibility pressures (MMPs) with the rising-bubble apparatus (RBA). *Fuel* **2016**, 175, 172–181.
59. Ge D, Cheng H, Cai M, Zhang Y, Dong P. A new predictive method for CO_2-Oil minimum miscibility pressure. *Geofluids* **2021**, 2021, 8868592.